Indian Journal of Chemical Technology
Vol. 31, September 2024, pp. 792-802
DOI: 10.56042/ijct.v31i5.3531

Studies on Ni(II) removal from industrial wastewater by magnetic activated carbon nanocomposite

Swaminathan Sribharathi[1], Gurusamy Kavitha[2]*, Ramasamy Sudha[3] & Ganeshan Dinesh Kumar[2]

[1]Department of Chemistry, Mahendra Arts and Science College (Autonomous), Namakkal 637501, Tamil Nadu, India
[2]Department of Chemistry, Gobi Arts & Science College, Gobichettipalayam 638 453, Tamil Nadu, India
[3]Department of Chemistry,Vivekanandha College of Arts and Sciences for Women(Autonomous), Tiruchengode 637 205, Tamil Nadu, India

*E-mail: shankaviya1980@gmail.com

Received 02 July 2023; Accepted 21 August 2024

A novel and effective bio-adsorbent based on magnetic activated carbon nanocomposites (MCHLAC) has been created from *citrus hystrix* leaves (CHL) as agricultural waste and then utilised for Ni(II) removal. Different parameters such as contact duration, metal ion concentration, pH, adsorbent dosage and temperature are optimised for the removal of Ni(II) metal. The FTIR, SEM, EDX, BET and TEM analysis are used to investigate the functionality, surface morphology, and elemental structure of CHL and MCHLAC. The adsorption isotherms fit well to Langmuir model and the maximum adsorption capacities of CHL and MCHLAC was 40.17 and 420.75 mg g^{-1}, respectively. Kinetic studies show that the CHL and MCHLAC are well fitted with the pseudo-second-order due to surface processes involving chemical adsorption of Ni(II) ions. Furthermore, the thermodynamic analysis of the process reveals that Ni^{2+} ion adsorption by the produced magnetic activated carbon is exothermic and spontaneous. According to the adsorption-desorption results, the MCHLAC can be used up to five cycles with excellent efficiency. As a result, the findings indicate that the magnetic nanocomposite loaded activated carbon, which demonstrated high efficiency, could be an effective option for a long-term water purification.

Keywords: *Citrus hystrix* leaves, Desorption, Kinetics, Magnetic nanocomposite, Nickel(II) removal

Introduction

Environmental pollution is the main factor that is adversely influencing human health. Many nations throughout the world lack the water needed to meet both human and ecosystem water needs as a result of industrial and population growth[1]. There are many causes of pollution, but two important ones are natural and human-made. The wastewater from industrial establishments makes up the majority of wastewaters that contain a variety of harmful metal ions. One of the most prevalent pollutants in wastewater is heavy metals, and numerous government agencies have implemented severe environmental regulations on these wastewater discharges[2]. One of the toxic heavy metal pollutants among the various heavy metals is Ni(II), which is released into wastewater during a variety of industrial processes, such as the manufacturing of steel, batteries, metal plating, smelting, and electronics[3]. The presence of Ni(II) in drinking water above the allowable limit (3 mg L^{-1}) can cause headaches, nausea, dizziness and vomiting, as well as chest pain, rapid respiration, cyanosis, and extreme weakness[4]. Because of the toxic effects of this metal, removing it from water and wastewater is critical for public health and the environment.

Numerous strategies for removing heavy metals from wastewaters have been researched in recent years, including chemical oxidation, membrane processes, coagulation, solvent extraction, ion exchange, distillation, biological treatment, reverse osmosis, and electrochemical methods[5-8]. Adsorption, which is one of numerous treatment methods used, is the safest since it is simple to use, effective at purifying, inexpensive, and ecologically acceptable. A variety of adsorbent materials are used to remove heavy metals from wastewater, including activated carbon, clays, chitosan, zeolites, and agricultural waste[9]. The development of magnetic nanoparticle-loaded activated carbon from a variety of agricultural wastes, including oyster shell[10], animal bone waste[11], palm kernel shell[12], corncob[13], palm oil shells[14], prawn shell[15], peanut shell[16], oak shell[17], *cucumismelo* peel[18], pomegranate[19], plum stone[20] have been successfully used for the removal of heavy metals form aqueous solution and wastewater.

Citrus hystrix leaves (CHL) is a kind of economical, environmentally friendly, abundant agricultural waste which is available in large amount. The synthesis of nanocomposite from agricultural waste provides unique physiochemical properties such as high surface area, mechanical and thermal properties, and is expected to influence the sorption capacity and increase the removal efficiency of heavy metals[21].

The objective of this study is to prepare the adsorption potential of new environmentally acceptable a magnetically loaded activated carbon sorbent developed from agricultural waste such as CHL to remove Ni(II) ions from aqueous solution. The adsorbent was characterized by using various techniques like FTIR, SEM, EDX, BET and TEM. The impact of several parameters, including contact time, adsorbent dosage, pH, and the initial concentration of Ni(II) ions, was investigated. Adsorption isotherms and kinetics were tested and evaluated the possible adsorption mechanism. Furthermore, the exothermic, spontaneity, and reusability of the nanocomposite were evaluated.

Experimental Section

Synthesis of *citrus hystrix* leaves (CHL) powder

Citrus hystrix leaves were collected from the local area in Namakkal district, Tamil Nadu, India, and washed carefully with deionised water to remove dust particles and other impurities. The collected raw materials was dried in a hot air oven at 100℃ for 8 h and crushed into powder and stored in a bottle.

Preparation of magnetic *citrus hystrix* leaves based activated carbon (MCHLAC)

About, 12 g of anhydrous ferric chloride ($FeCl_3$) and 6 g of hydrated ferrous chloride ($FeCl_2.6H_2O$) were mixed in 200 mL of distilled water and stirring vigorously at 80℃ for 30 min. Then 10 g of CHL powder was added and the solution was stirred for 1 h. Then 20 mL of 25 % NaOH solution was added drop wise and stirring was continued until the black coloured precipitate was obtained. The precipitate was filtered and dried at 100℃ for 12 h. The resultant impregnated samples were activated at 350℃ for 3 h in a muffle furnace. After cooling, the activated sample were washed with deionised water until the pH of the filtrate was about 6-7, and dried in a hot air oven for 6 h at 110℃. The obtained samples were named as magnetic *citrus hystrix* leaves based activated carbon (MCHLAC) and stored in a bottle then used for further experiments.

Preparation of Ni(II) solutions

The stock solution of Ni(II) ions (1000 ppm) were prepared by dissolving 4.479 g of nickel sulphate in 1000 mL of distilled water. For pH adjustment HCl and NaOH solution (0.1– 1 M) were used. The nickel containing industrial wastewater was collected from M S plates in Perundurai in Erode district, India.

Batch adsorption experiments

Batch adsorption studies have been carried out in plastic bottles of 300 mL capacity containing 100 mL of 20 mg L^{-1} initial Ni(II) concentration and 100 mg of adsorbent at pH 7.0. Then the reaction mixture was shaken in a temperature controlled shaker at a constant speed of 200 rpm at room temperature for changing the time for various intervals. The influence of solution pH was identified by adjusting the pH to a specific value by using 0.1 N of HCl/NaOH solutions. The isotherm studies were conducted varying the initial Ni(II) concentration as 10-60 mg L^{-1} at 27, 37, 47 ℃. The kinetic studies were conducted for the Ni(II) concentrations over the range of 20 mg L^{-1} at an optimum pH and at room temperature. Each experiment was carried out more than once, and the average results are taken in this work. After the equilibrium period, the content was centrifuged, filtered, and an atomic absorption spectrophotometer (Elico Model-SL 163) was used to measure the quantities of Ni(II) ions.The percentage removal of nickel(II) and adsorption capacity was estimated under the following Eqs (1) and (2):

$$\% \text{ Removal of nickel} = \frac{C_0 - C_e}{C_0} \times 100 \quad \ldots (1)$$

$$\text{Adsorption capacity } (q_e) = \frac{C_0 - C_e}{M} \times V \quad \ldots (2)$$

where C_e and C_o are the equilibrium and initial concentrations of Ni(II) (mg L^{-1}); V is the volume of Ni(II) solution (L); M is the mass of the adsorbent used (g); q_e is the adsorption capacity at equilibrium (mg g^{-1}), respectively.

Results and Discussion

Fourier transforms infrared spectroscopy studies

The effect of nickel ion adsorption on the surface functional groups of the synthesized adsorbent was investigated using FTIR analysis in the spectrum range of 400-4000 cm^{-1} and the results are presented in Fig. 1 (a) & (b).The bands within the range of 3448

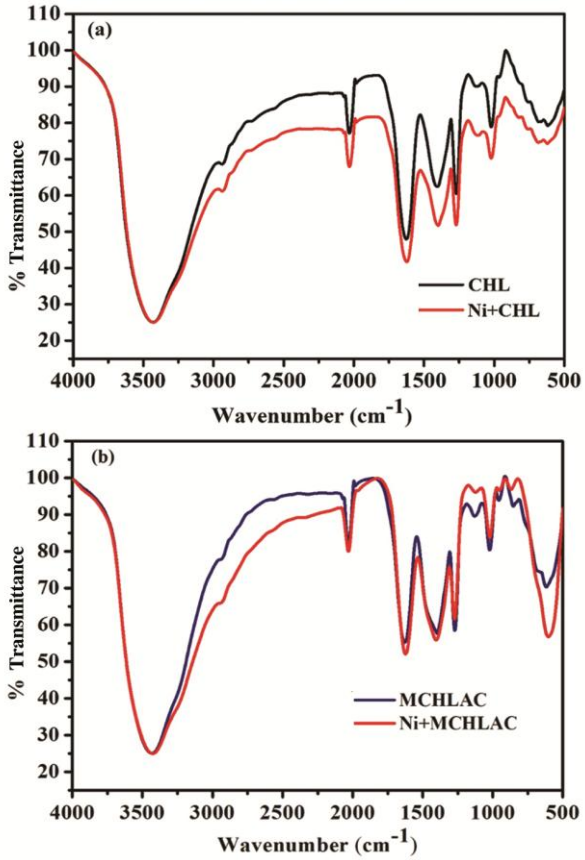

Fig. 1 — FTIR spectra of (a) CHL & Ni+ CHL and (b) MCHLAC & Ni+MCHLAC

-3474 cm^{-1} correspond to OH group (alcohols, phenols and carboxylic acids) which is accountable for the metal binding process in CHL and MCHLAC[22]. The peak at about the range of 2922-2924 cm^{-1} denotes the aliphatic C-H groups[23]. The peaks observed at 1701-1744 cm^{-1} could be designated the C=O stretching vibration of carboxyl groups[24]. At the same time as comparing the both raw and magnetic activated carbon, there are various functional group values are shifted on the surface of MCHLAC and Fe-O group is observed at a frequency of 551.64 cm^{-1} (Ref. 25, 26). The FTIR spectrum of Ni(II) ions loaded CHL and MCHLAC shows that the peaks are shifted slightly from their original arrangement and their values of intensity are also distorted. From the above results clear that the hydroxyl and carboxylic acid groups in CHL, in addition to that Fe-O groups are present in MCHLAC, which is responsible for the adsorption of Ni(II) ions.

Scanning electron microscopy (SEM), Energy dispersive X- ray spectroscopy (EDAX) studies, BET and TEM analysis

SEM analysis was used to analyse the surface modifications of the present adsorbent before and after the treatment. SEM images of CHL and MCHLAC before and after the adsorption of nickel(II) ions are shown in Figs 2 (a)-(d). The adsorbent surface has pores, ripplings, and holes, which increase its specific surface area and vacant

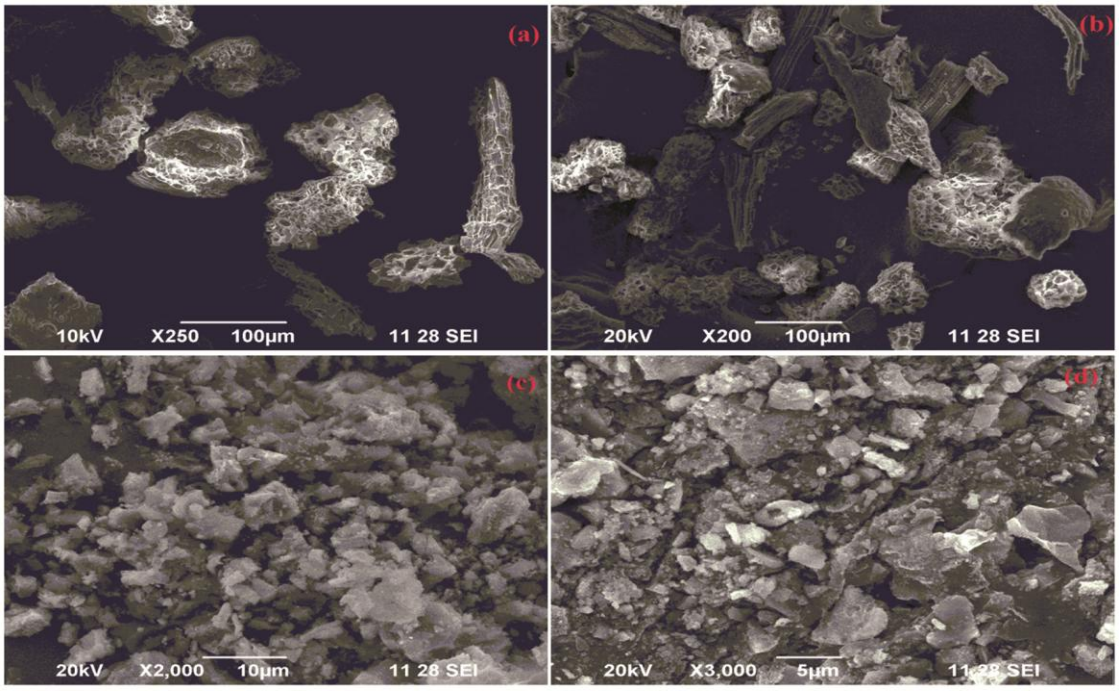

Fig. 2 — SEM images of (a) CHL, (b) Ni+ CHL, (c) MCHLAC and (d) Ni+MCHLAC

active sites for nickel ion adsorption (Fig. 2a & c). Furthermore, the majority of the surface pores were occupied and covered by the adsorbed Ni(II) ions after the adsorption process (Fig. 2b & d).

EDX analysis of the CHL and MCHLAC before and after the adsorption of Ni(II) ion is shown in Figs 3 (a)-(d). The elemental analysis of the CHL and MCHLAC surface is determined by EDX showed that the presence of Ca and Fe (Fig. 3c) are considered to be an effective binding adsorption sites. According to the EDX result in Fig. 3 (d) after the nickel(II) adsorption, the Ca and Fe elements containing peaks are vanished and are replaced by Ni(II). This could be indicated that the presence of Ni(II) ion through metal binding process which is confirmed by EDX analysis.

The specific surface area, average pore diameter and pore volume were analysed by BET (Fig. 4) was 95.152 m^2 g^{-1}, 2.685 nm and 0.124 cc g^{-1},respectively, which showed that the surface was smooth, irregular which supported the adsorption process. This high surface area of adsorbent's surface is more effective for the elimination of Ni(II) ion. TEM micrographs as shown Fig. 5 revealed the presence of nearly spherical iron oxide nanoparticles deposited on mesoporous carbon nanolayer. The average particles size is calculated to be 6 nm. Fig. 5 (b) shows that HRTEM profile of iron oxide core on carbon nanolayer and interlayer distance is found to be 0.213 nm. The dispersion of magnetic particles on the magnetic activated carbon surfaces would influence the ease of aqueous ion access to surface active sites of the carbon and to some pores. Thus, the number of sites available for Ni^{2+} adsorption, and thereby the kinetic and equilibrium behaviour of the adsorption process, are influenced.

Influence of contact time and initial metal ion concentration

Contact time is a significant factor in determining adsorption kinetics. Percentage removal of Ni(II) ions was calculated as a function of agitation time (30-180 min) and initial Ni(II) concentrations (20- 40 mg L^{-1}) at pH 7.0 and constant CHL and MCHLAC dose

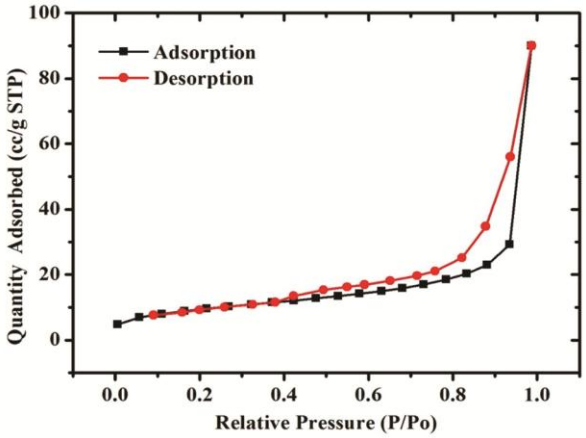

Fig. 4 — BET-BJH analysis for synthesised MCHLAC

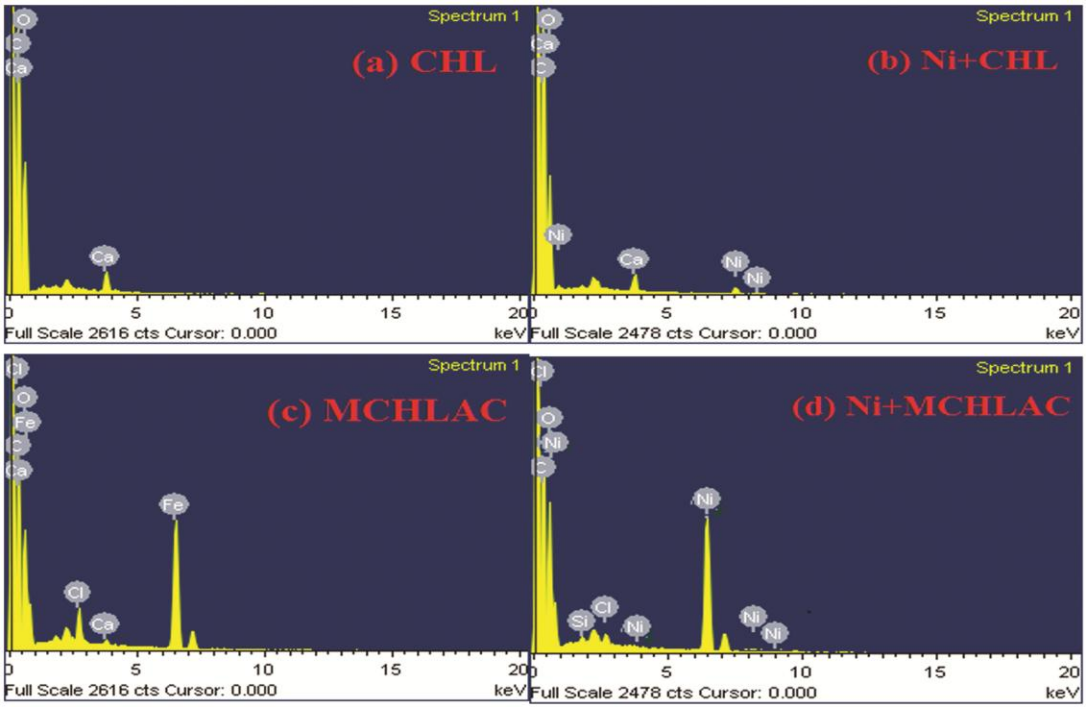

Fig. 3 — EDX images of (a) CHL, (b) Ni+ CHL, (c) MCHLAC and (d) Ni+MCHLAC

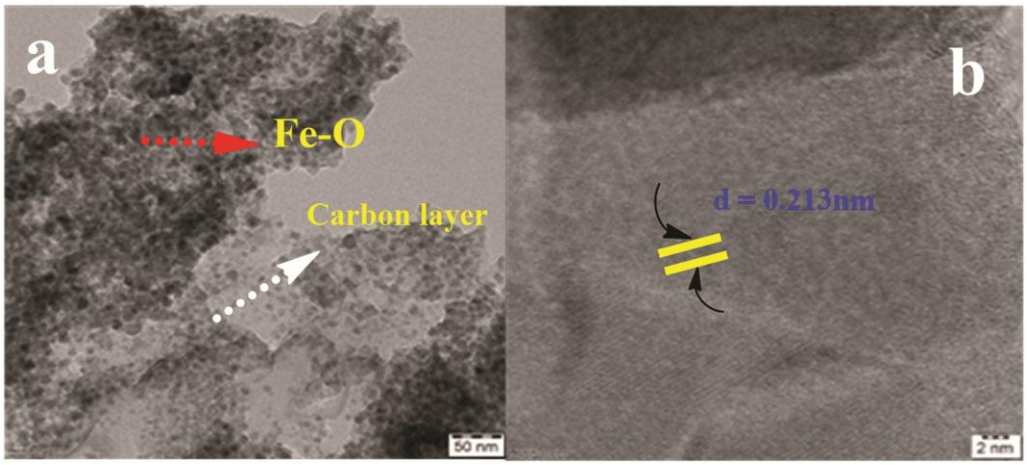

Fig. 5 — (a) TEM profile (b) HRTEM profile for synthesised MCHLAC

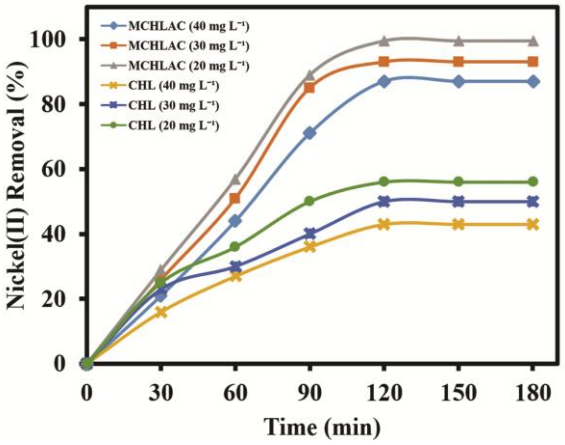

Fig. 6 — Effect of contact time for removal of Ni(II) ions at different concentrations of Ni(II) ions

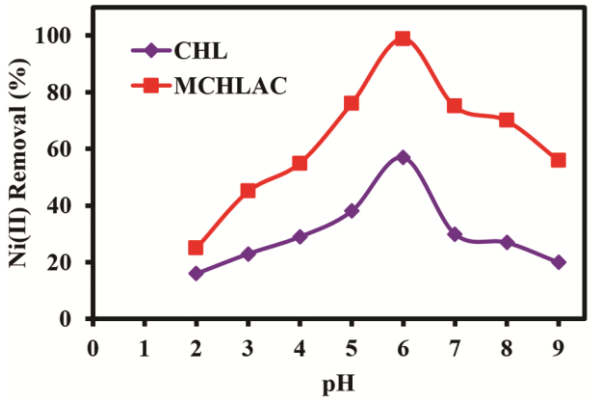

Fig. 7 — Effect of solution pH for removal of Ni(II) ions

of 100 mg. Fig. 6 shows that the percentage of Ni(II) elimination reached a maximum within 120 min and then remained relatively unchanged. The rapid removal efficiency during the first 120 min could be attributed to availability of free active sites at the adsorbent surfaces gradually occupied with time by metal ions. As the binding sites became exhausted, the uptake rate slowed down due to competition for decreasing availability of actives sites by metal ions. Hence, the optimal contact time was found to be 120 min and maintained for further experiments. Secondly, the Ni(II) removal capacity decreased with increasing initial Ni(II) concentrations. At higher concentration, the availability of Ni(II) ions are more which in turn might provide higher driving force is supplied for the metal ions from the solution to the sorbents.

Influence of solution pH

Solution pH is thought to be one of the most important environmental factors in determining the value of primary application of an adsorbent since it affects the surface charge of the material, its capacity for adsorption, and the kinds of heavy metal ions that are present in aqueous solutions. Fig. 7 illustrates the results of a study that examined the impact of pH on the removal of Ni(II) ions from aqueous solution onto CHL and MCHLAC throughout a pH range of 2–10. At low pH values, H^+ ions occupy most of the adsorption sites on the adsorbent surface and less nickel could be adsorbed because of electric repulsion with H^+ ions on adsorbent surface. When the pH value increases, adsorbent surface is more negatively charged and the adsorption of Ni(II) ions increased and reached maximum removal at pH 6.0. The decrease in adsorption efficiency at higher pH (>6.0) was due to the formation of soluble hydroxylated complexes of the nickel ions and their competition with the active sites as a result, the retention would decrease again[28]. This is because the creation of nickel hydroxide reduces the likelihood that free Ni(II) ions exist in the basic medium[27, 28]. Hence, an

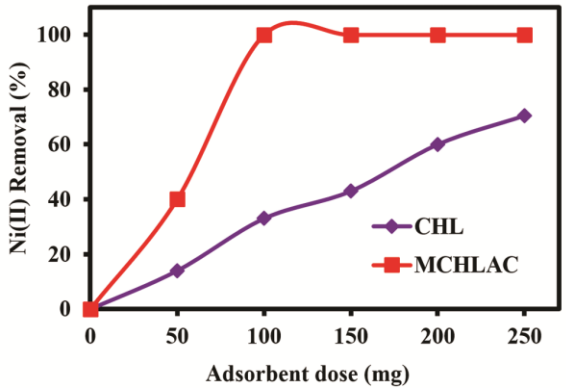

Fig. 8 — Effect of adsorbent dose for removal of Ni(II) ions

optimum pH value of 6.0 was fixed for further studies. The possible sorption mechanism that may takes place at different pH condition represented as follows:

$$MCHLAC–OH \longleftrightarrow MCHLAC–O^- + H^+$$
$$MCHLAC – O^- + Ni^{2+} \longleftrightarrow MCHLAC – O – Ni$$

Influence of CHL and MCHLAC dose

The effect of CHL and MCHLAC dose of 50-250 mg on the elimination of Ni(II) removal was tested by a Ni(II) concentration of 20 mg L^{-1} at pH 6.0. Fig. 8 shows that increasing the doses of CHL and MCHLAC from 50-250 mg and 50-100 mg, respectively, enhanced the uptake of Ni(II) ions, but after that the removal percentage remained constant and reached its maximum removal of 70. 5 ± (0.4) and 99.4 ± (0.3) % at 0.25 and 0.1 g, respectively. Increasing the dosage of CHL and MCHLAC could increase adsorption sites and bring more available exchangeable sites, resulting in increased removal of Ni(II) ions from aqueous solutions by CHL and MCHLAC.

Studies on adsorption isotherm and thermodynamic process

Adsorption isotherms are frequently used to predict the effectiveness of sorbents and the nature of their interactions with contaminants[29]. These models might reveal details about the adsorption capabilities and surface characteristics of adsorbents. The adsorption data were characterised, investigated, and modelled using several isotherms linking Ni(II) adsorption per unit mass of the adsorbent to arrive at equilibrium concentrations of Ni(II) pollutants. In this work, the equilibrium data of potentially hazardous metal ions, namely Ni(II) ions, were compared with three different isotherm models at different temperatures, including Langmuir[30], Freundlich[31], Dubinin-Radushkevich[32], Temkin[33], and Sips[34] in order to discover the best fitting model. The Langmuir, Freundlich, Dubinin-Radushkevich, Temkin, and Sips models are expressed as the following Eqs. 1, 2, 3, 4 and 5, respectively.

$$q_e = \frac{q_m K_L C_e}{1+K_L C_e} \quad \text{... (1)}$$

$$q_e = K_F C_e^{1/n} \quad \text{... (2)}$$

$$q_e = q_{mD}\, e^{-\beta\varepsilon^2} \quad \text{... (3)}$$

$$q_e = B \ln(AC_e) \quad \text{... (4)}$$

$$q_e = q_{max}\frac{K_s C_e^{\gamma}}{1+K_s C_e^{\gamma}} \quad \text{... (5)}$$

$$R_L = \frac{1}{1+K_L C_0} \quad \text{... (6)}$$

$$\varepsilon = RT\ln[1+\frac{1}{C_e}] \quad \text{... (7)}$$

$$E = [\frac{1}{\sqrt{2\beta}}] \quad \text{... (8)}$$

Where q_m, K_L, K_F, n, A, B, q_{mD}, β and E are the isotherm parameters of these models. The results of the isotherm constants, such as correlation coefficients (R^2), sum of squares error (SSE) and root mean squared error (RMSE), were determined from the plot of q_e versus C_e (Figs. 9a and b), and these are shown in Table 1. As summarized in Table 1, the results shows that the better fitting of the data by the Langmuir model compared with other five isotherm models based on the greater R^2 values and small SSE, RMSE values. This observation confirms the homogeneous monolayer coverage of Ni(II) ions onto CHL and MCHLAC. The maximum monolayer adsorption capacity of Ni(II) ions onto MCHLAC was found to found to be 420.75 mg g^{-1}, which was about 10.5 times greater than that of CHL (40.17 mg g^{-1}). From this study, the uptake of Ni(II) ions onto CHL and MCHLAC from aqueous medium is decreased with increasing temperature indicating that the adsorption process is exothermic in nature.

Thermodynamic parameters were established at various temperatures (298 to 328 K) to assess the adsorption capacity of Ni(II) ions onto CHL and MCHLAC. (Fig. 10a). As shown in Fig. 10a, rising temperature causes a rise in q_e, indicating that the process of adsorption thermodynamic is exothermic. Furthermore, the findings from Fig.10b and Table 1 indicated that the adsorption process was spontaneous and thermodynamically favourable under the

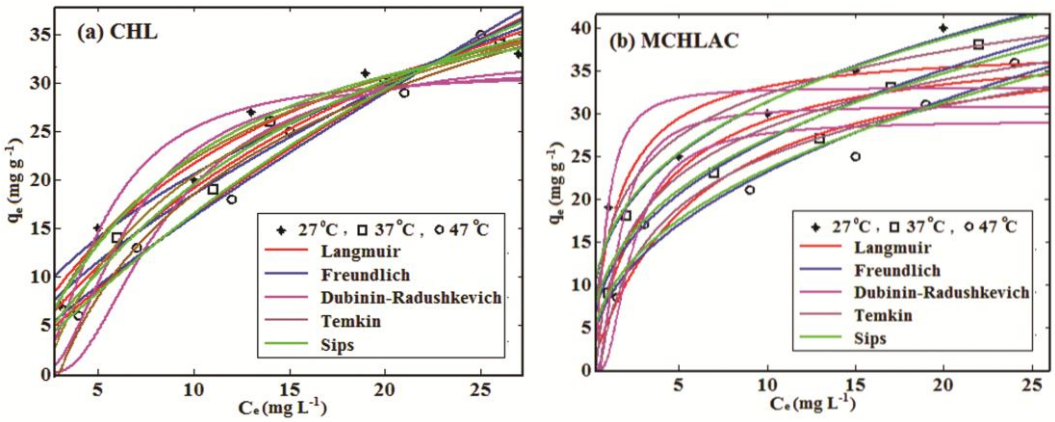

Fig. 9 — Nonlinear isotherm for the elimination of Ni(II) ions by (a) CHL and (b) MCHLAC

Table 1 — Nonlinear equilibrium isotherm factors and thermodynamic parameters for the removal of Ni(II) ions

Isotherm model	Parameters	CHL			MCHLAC		
		27°C	37°C	47°C	27°C	37°C	47°C
Langmuir	q_m (mg g^{-1})	40.17	38.91	35.83	420.75	370.45	330.36
	K_L (L mg^{-1})	0.700	0.299	0.162	0.453	0.382	0.290
	RMSE	3.593	3.761	3.976	1.503	1.576	1.986
	R^2	0.990	0.991	0.992	0.991	0.990	0.991
	SSE	51.63	56.59	63.22	15.77	18.99	20.67
Freundlich	K_F (mg g^{-1})	5.801	3.888	2.370	15.28	11.06	8.295
	n (g L^{-1})	1.819	1.475	1.197	3.210	2.597	2.244
	RMSE	2.917	2.101	1.616	2.505	2.598	2.550
	R^2	0.933	0.924	0.919	0.941	0.937	0.925
	SSE	10.44	17.66	34.04	25.10	27.00	26.07
Dubinin-Radushkevich	q_{mD} (mg g^{-1})	21.67	20.58	18.32	32.64	28.25	26.54
	β x 10^{-7} ((mol.K kJ^{-1})^2)	3.875	3.786	3.467	1.434	1.316	1.487
	E (kJ mol^{-1})	1.136	1.149	1.200	1.867	1.949	1.834
	RMSE	3.331	3.654	4.036	5.224	5.327	5.243
	R^2	0.887	0.879	0.866	0.822	0.767	0.792
	SSE	65.15	53.42	44.39	89.56	78.40	64.36
Temkin	A (L mg^{-1})	0.629	0.446	0.334	9.077	3.311	1.841
	B	5.231	5.922	6.601	3.106	3.509	3.711
	RMSE	1.719	1.513	2.234	2.750	3.025	3.144
	R^2	0.964	0.924	0.912	0.945	0.933	0.910
	SSE	11.83	15.44	16.78	30.25	36.59	39.53
Sips	q_{max}(mg g^{-1})	49.92	39.63	32.40	157.4	132.3	111.3
	K_s (L/mg)	0.298	0.107	0.030	0.542	0. 432	0.110
	γ	2.314	1.567	1.175	0.306	0.364	0.421
	RMSE	1.974	1.636	1.705	2.905	3.079	3.029
	R^2	0.927	0.918	0.929	0.959	0.948	0.944
	SSE	11.69	8.028	8.719	25.32	28.45	27.52
Thermodynamic	ΔG^0 (kJ mol^{-1})	-12.745	-5.662	-4.220	-1.115	-0.622	-0.213
	ΔH^0 (kJ mol^{-1})		-15.306			-151.057	
	ΔS^0 (kJ mol^{-1}K^{-1})		-0.047			-0.461	

experimental circumstances due to the negative enthalpy and entropy change.

The adsorptions capacities of CHL and MCHLAC towards Ni^{2+} have been compared with various adsorbents reported in the literature and are listed in Table 2. It could be concluded that the monolayer adsorption capacity is comparable to other researcher's results. It showed that MCHLAC has a promising adsorbent for the removal of Ni(II) ions from aqueous solutions.

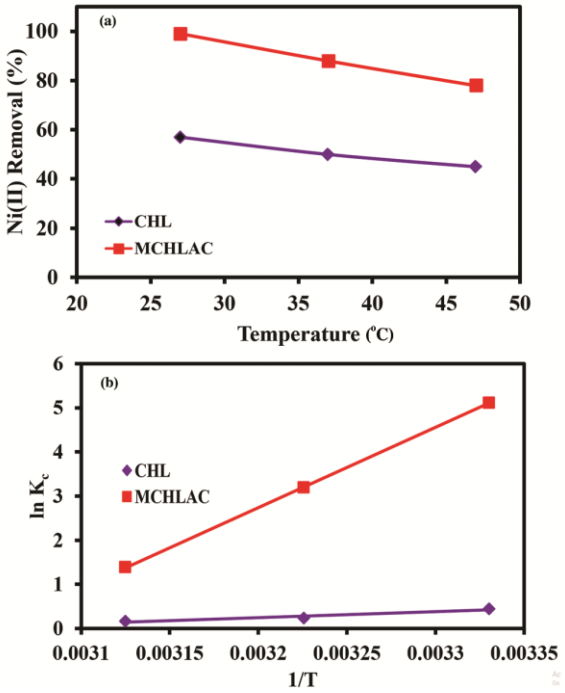

Fig. 10 — (a) Effect of temperature and (b) thermodynamic diagrams for removal of Ni(II) ions

Table 2 — Langmuir monolayer adsorption isotherm capacities compared with other adsorbents reported from the literature for the removal of Ni(II) ions

Adsorbents	Adsorption capacity ($q_m$mg g^{-1})
Sunflower seed husk[35]	79.37
Coffee husk (HAC)[36]	57.14
Passion fruit shell[37]	182.67
Palm kernel shell[38]	40.00
Pongamiapinnata shell[39]	192.00
Lemon and orange seeds[40]	118.02
Mespilusgermanica leaf[41]	13.08
Walnut green peel[42]	129.00
Palm kernel chaff[43]	120.60
Citrus limetta leaves[44]	58.14
Azadirachtaindica leaf[45]	120.60
CHL (Present Study)	**40.17**
MCHLAC (Present Study)	**420.75**

Adsorption kinetics

The pseudo-first-order model is predicated on the idea that the adsorbate's dispersion regulates the rate of adsorption. The chemical adsorption step is assumed by the pseudo-second-order model to be the rate-limiting step owing to interactions at the surface of the adsorption layer. In this research, the pseudo-first-order[46], pseudo-second-order models[47], elovich[48] and fractional power equation were applied with the following mathematical forms to assess the adsorption of Ni(II).

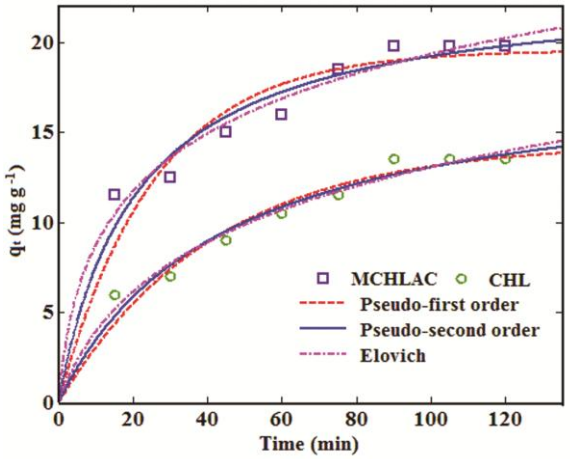

Fig. 11 — Nonlinear kinetic models for the elimination of Ni(II) ions

Table 3 — Kinetic constants for the elimination of Ni(II) ions

Kinetic model	Parameters	CHL	MCHLAC
Pseudo-first order	k_1(min^{-1})	0.024	0.039
	$q_{e,}$ cal (mgg^{-1})	12.34	15.67
	R^2	0.930	0.940
	SSE	14.82	16.46
	RMSE	1.549	0.845
Pseudo-second order	k_2 (g $mg^{-1}min^{-1}$)	0.001	0.002
	$q_{e,}$cal (mg g^{-1})	14.39	19.53
	$q_{e,}$exp(mg g^{-1})	14.50	19.50
	R^2	0.990	0.991
	SSE	8.082	9.879
	RMSE	0.567	0.435
Elovich	α	0.091	0.415
	β	1.251	1.156
	R^2	0.959	0.941
	SSE	12.54	5.758
	RMSE	0.651	0.557

$$q_t = q_e(1-\exp k_1 t) \quad \text{... (9)}$$

$$q_t = k_2 q_e^2 t / (1 + k_2 q_e t) \quad \text{... (10)}$$

$$q_t = \beta(\ln\alpha\beta) + \beta(\ln t) \quad \text{... (11)}$$

where q_t and q_e (mg g^{-1}) are the adsorption capabilities at time t and equilibrium (min), whereas k_1 and k_2 are the pseudo-first-order (min^{-1}) and pseudo-second-order (g mg^{-1} min^{-1}) equilibrium rate constants, α is the starting rate of adsorption (mg g^{-1} min^{-1}), β is the adsorption constant in relation to the available adsorption sites (g mg^{-1}).

The kinetic parameters calculated from Eqs. 9, 10 and 11 are listed in Table 3 and shown in Fig. 11. In spite of this, the q_e value that was calculated using Eq. 9 does not concur with the q_e experimental value. Additionally, it appears that the adsorption of Ni(II)

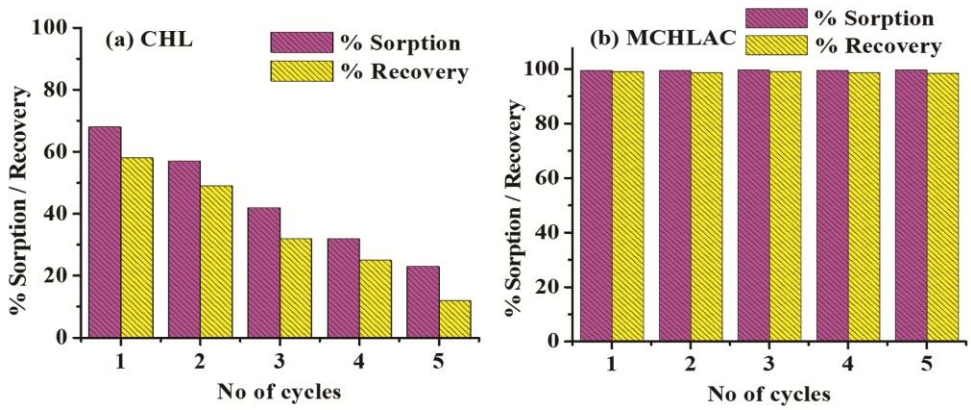

Fig. 12 — Regeneration and recycling by batch process for the removal Ni(II) ions onto (a) CHL and (b) MCHLAC

ions does not follow the pseudo-first-order kinetics, based on the correlation value of the pseudo-second-order kinetic model (R^2 = 0.999). According to the aforementioned findings, the adsorption kinetics of Ni(II) on CHL and MCHLAC can be satisfactorily fitted by pseudo-second-order kinetics; therefore, chemisorption mechanism could regulate the overall rates of the adsorption process. It is also worth noting that the experimental findings agree well with the data from the central composite design model.

Desorption study

A perfect adsorbent for practical application should be able to recover and retain its initial absorption capacity while also being to produce cost-effective. In this study, metal ions from CHL and MCHLAC are extracted using an external magnetic field and then rinsed off with distilled water. The absorbent was then treated with a 0.1 M HCl solution to extract the metal ions from it.The renewed adsorbents were dried in an oven at 70°C for 2 h before being used in a number of adsorption-desorption tests. The recovered adsorbents were used for the adsorption-desorption cycle at five times, and the results are presented in Figs 12a and b. The high value of sorption (98.0 - 99.0 %) may observed because of additional surface active sites present on the sorbent surface open after repeated regeneration cycles. For CHL, both the adsorption and desorption values decreased rapidly, because the Ni(II) ions were strongly bound to the new opening sites[49]. The results showed that MCHLAC was a very effective adsorbent for Ni(II) ions, absorbing up to 99% after five times without losing an adsorption capacity as that of CHL.

Conclusion

Magnetic *Citrus hystrix* leaves based activated carbon was effectively synthesised from *Citrus hystrix* leaves and used as a low-cost, reusable adsorbent for extracting Ni(II) ions from aqueous medium. The Ni (II) removal results revealed that the highest adsorption effectiveness of MCHLAC was 99.3± 0.4 % at pH = 6.0, adsorbent dosage of 100 mg, contact duration of 90 min, temperature of 27°C, and starting ion concentration of 20 mg L^{-1}. The adsorption isotherms were described using the five models, with the Langmuir model providing the best fitting and the highest adsorption capacity was determined to be 420.75 mg g^{-1}. The kinetics investigations showed that the experimental data could be well matched by the quasi second-order rate equation. Furthermore, thermodynamic tests showed that the adsorption process was exothermic and spontaneous. According to the experimental findings, the MCHLAC adsorbent had several benefits, including high adsorption characteristics, high efficiency, low cost, and good reusability. As a result, the MCHLAC adsorbent can be presented as an appropriate adsorbent for removing nickel(II) ions from industrial wastewater.

References

1 Bond N R, Burrows R M, Kennard M J & Bunn S E, Water scarcity as a driver of multiple stressor effects, *Multi Stress River Ecosystem*, (2019) 111.

2 Unlu N & Ersoz M, Adsorption characteristics of heavy metal ions onto a low cost biopolymeric sorbent from aqueous solutions, *J Hazard Mater*, 136 (2006) 272.

3 Khedri A, Jafari D & Esfandyari M, Adsorption of nickel(II) ions from synthetic wastewater using activated carbon prepared from *Mespilus germanica* leaf, *Arab J Sci Eng*, 47 (2022) 6155.

4 Kalaivani S S, Vidhyadevi T, Murugesan A, Baskaralingam P, Anuradha C D & Ravikumar L, Equilibrium and kinetic studies on the adsorption of Ni(II) ion from an aqueous solution using activated carbon prepared from the Obroma cacao (cocoa) shell, *Desalin Water Treat*, 54 (2015) 1629.

5 Doyurum S & Çelik A, Pb(II) and Cd(II) removal from aqueous solutions by olive cake, *J Hazard Mater*, 138 (2006) 22.

6 Gupta S & Babu B V, Removal of toxic metal Cr(VI) from aqueous solutions using sawdust as adsorbent: Equilibrium, kinetics and regeneration studies, *Chem Eng J*, 150 (2009) 352.

7 Salah T A, Mohammad A M, Hassan M A & El-Anadouli B E, Development of nano-hydroxyapatite/chitosan composite for cadmium ions removal in wastewater treatment, *J Taiwan Inst Chem Eng*, 45 (2014) 1571.

8 Sani H A, Ahmad M B & Saleh T A, Synthesis of zinc oxide/talc nanocomposite for enhanced lead adsorption from aqueous solutions, *RSC Adv*, 6 (2016) 108819.

9 Sudha R & Srinivasan K, Nickel(II) removal using modified *Citrus limettioides* peel, *Int J Environ Sci Technol*, 12 (2015) 3993.

10 Wu S, Liang L, Zhang Q, Xiong L, Shi S, Chen Z, Lu Z & Fan L, The ion-imprinted oyster shell material for targeted removal of Cd(II) from aqueous solution, *J Environ Manag*, 302 (2022) 114031.

11 Prabu D, Kumar P S, Rathi B S, Sathish S, Anand K V, Kumar J A, Mohammed O B & Silambarasan P, Feasibility of magnetic nano adsorbent impregnated with activated carbon from animal bone waste: Application for the chromium(VI) removal, *Environ Res*, 203 (2022) 111813.

12 Michael J J, Edinsha G E H & Joseph J, Nanoporous palm kernel shell as an effective adsorption for the treatment of lead ion from contaminated water, *ECS Trans*, 107 (2022) 18753.

13 Kamal K H, Attia M S, Ammar N S & Abou-Taleb E M, Kinetics and isotherms of lead ions removal from wastewater using modified corncob nanocomposite, *Inorg Chem Commun*, 130 (2021) 108742.

14 Buhani B, Suharso S, Mita R, Miranda S & Sumadi S, Removal of Cd(II) ions in solution by activated carbon from palm oil shells modified with magnetite, *Desal Water Treat*, 218 (2021) 352.

15 Guo J, Song Y, Ji X, Ji L, Cai L, Wang Y, Zhang H & Song W, Preparation and characterization of nanoporous activated carbon derived from prawn shell and its application for removal of heavy metal ions, *Materials (Basel)*, 12 (2019) 241.

16 Cai W, Li Z, Wei J & Liu Y, Synthesis of peanut shell based magnetic activated carbon with excellent adsorption performance towards electroplating wastewater, *Chem Eng Res Design*, 140 (2018) 23.

17 Mousavi S M, Hashemi S A, Esmaeili H, Mohammed A A & Mojoudi F, Synthesis of Fe_3O_4 nanoparticles modified by oak shell for treatment of wastewater containing Ni(II), *Acta Chim Slov*, 65 (2018) 750.

18 Manjuladevi M, Krishnaveni J & Manomani S, Removal of nickel(II) from aqueous solution by adsorption onto nano adsorbent prepared from, *Cucumismelo* peel, *Int J Chem Tech Res*, 10 (2017) 337.

19 Salmani M H, Abedi M, Mozaffari S A & Sadeghian H A, Modification of pomegranate waste with irons a green composite for removal of Pb from aqueous solution: Equilibrium, thermodynamic and kinetic studies, *AMB Express*, 7 (2017) 225.

20 Parlayici S & Pehlivan E, Removal of metals by Fe_3O_4 loaded activated carbon prepared from plum stone *(Prunusnigra)*: Kinetics and modelling study, *Powder Technol*, 317 (2017) 23.

21 Hannah W & Thompson P B, Nanotechnology, risk and the environment: A review, *J Environ Monit*, 10 (2008) 291.

22 Aydin H, Bulut Y & Yerlikaya C, Removal of copper(II) from aqueous solution by adsorption onto low-cost adsorbents, *J Environ Manag*, 87 (2008) 37.

23 Malkoc E & Nuhoglu Y, Investigations of nickel(II) removal from aqueous solutions using tea factory waste, *J Hazard Mater*, B127 (2005) 120.

24 Feng N, Guo X & Liang S, Adsorption study of copper(II) by chemically modified orange peel, *J Hazard Mater*, 164 (2009) 1286.

25 Panneerselvam P, Morad N & Tan K A, Magnetic nanoparticle (Fe_3O_4) impregnated onto tea waste for the removal of nickel(II) from aqueous solution, *J Hazard Mater*, 186 (2011) 160.

26 Sribharathi S, Anitha P, Sudha R, Poornima K & Kavitha G, Cadmium(II) removal from aqueous solution using a novel magnetic nanoparticle impregnated onto *Citrus hystrix* leaves, *Desal Water Treat*, 196 (2020) 388.

27 Kalaivani S S, Vidhyadevi T, Murugesan A, Baskaralingam P, Anuradha C D, Ravikumar L & Sivanesan S, Equilibrium and kinetic studies on the adsorption of Ni(II) ion from an aqueous solution using activated carbon prepared from *Theobroma cacao* (cocoa) shell, *Desal Water Treat*, 54 (2015) 1629.

28 Sudha R, Srinivasan K & Premkumar P, Removal of nickel(II) from aqueous solution using C*itrus limettioides* peel and seed carbon, *Ecotoxicol Environ Safe*, 117 (2015) 115.

29 Ho Y S, Huang C T & Huang H W, Equilibrium sorption isotherm for metal ions on tree fern, *Process Biochem*, 37 (2002) 1421.

30 Langmuir I, The adsorption of gases on plane surfaces of glass, mica and platinum, *J Am Chem Soc*, 40 (1918) 1361.

31 Freundlich H M F, Over the adsorption in solution, *J Phys Chem*, 57 (1906) 385.

32 Temkin M J & Pyzhev V, Recent modifications to Langmuir isotherms, *Acta Physicochim URSS*, 12 (1940) 217.

33 Dubinin M M & Radushkevich L V, Equation of the characteristic curve of activated charcoal, *Chem Zentralbl*, 1 (1947) 875.

34 Sips R, On the structure of a catalyst surface, *J Chem Phys*, 16 (1948) 490.

35 Srisuwan W, Jubsilp C & Srisorrachatr S, The use of K_2CO_3 modified sunflower seed husks for removing of metal ions from industrial wastewater, *Chem Eng Trans*, 70 (2018) 241.

36 Rodiguez M H, Yperman J, Carleer R, Maggen J, Dadi D, Gryglewicz G, Bruggen B V D, Hernandez J F & Calvis A O, Adsorption of Ni(II) on spent coffee and coffee husk based activated carbon, *J Environ Chem Eng*, 6 (2018) 1161.

37 Paula-Ramos B D, Dias-Perez I, Silva-Paiano M, Adeodato-Vieira M G & Freire-Boina R, Activated carbons from passion fruit shells in adsorption of multimetal wastewater, *Environ Sci Pollut Res*, 29 (2022) 1446.

38 Baby R, Hussein M Z, Zainal Z & Abdullah A H, Functionalized activated carbon derived from palm kernel shells for the treatment of simulated heavy metal-contaminated water, *Nanomaterials*, 11 (2021) 3133.

39 Patra C, Shahnaz T, Subbiah S & Narayanasamy S, Comparative assessment of raw and acid-activated preparations of novel *Pongamiapinnata* shells for adsorption of hexavalent chromium from simulated wastewater, *Environ Sci Pollut Res*, 27 (2020) 14836.

40 Karapinar H S, Adsorption performance of activated carbon synthesis by $ZnCl_2$, KOH, H_3PO_4 with different activation temperatures from mixed fruit seeds, *Environ Technol*, 43 (2022) 1417.

41 Khedri A, Jafari D & Esfandyari M, Adsorption of nickel(II) ions from synthetic wastewater using activated carbon prepared from *Mespilusgermanica* leaf, *Arab J Sci Eng*, 47 (2022) 6155.

42 Yu M, Zhu B, Yu J, Wang X, Zhang C & Qin Y, A biomass carbon prepared from agricultural discarded walnut green peel: Investigations into its adsorption characteristics of heavy metal ions in wastewater treatment, *Biomass Convers Biorefin*, 13 (2022) 1.

43 Nnaji C C, Agim A E, Mama C N, Emenike P G C & Ogarekpe N, Equilibrium and thermodynamic investigation of biosorption of nickel from water by activated carbon made from palm kernel chaff, *Sci Rep*, 11 (2021) 7808.

44 Aboli E, Jafari D & Esmaeili H, Heavy metal ions (lead, cobalt and nickel) biosorption from aqueous solution onto activated carbon prepared from *Citrus limetta* leaves, *Carbon Lett*, 30 (2020) 683.

45 Patel H, Batch and continuous fixed bed adsorption of heavy metals removal using activated charcoal from neem (*Azadirachtaindica*) leaf powder, *Sci Rep*, 10 (2020) 16895.

46 Lagergren S, Zur theorie der sogenannten adsorption geloster stoffe, *Kungliga Svenska Vetens kapsakad Handl*, 24 (1898) 1.

47 Ho Y S, Second order kinetic model for the sorption of cadmium onto tree fern: A comparison of linear and nonlinear methods, *Water Res*, 40 (2006) 119.

48 Thajeel A S, Modeling and optimization of adsorption of heavy metal ions onto local activated carbon, *Aqua Sci Technol*, 1 (2013) 108.